Animal Nutrition 20 (2025) 263–276

Contents lists available at ScienceDirect

Animal Nutrition

journal homepage: http://www.keaipublishing.com/en/journals/aninu/

Original Research Article

Undernutrition disrupts jejunal and ileal microbiota and epithelial tissue homeostasis in a pregnant sheep model

Weibin Wu [a, †], Muhammad Faheem Akhtar [b, †], Jiahong Geng [a, †], Huizhen Lu [c], Muhammad Ajwad Rahim [a], Jianbo Cheng [a], Xiaoling Ding [a], Shengyong Mao [d, *], Yanfeng Xue [a, *]

[a] College of Animal Science and Technology, Anhui Agricultural University, Hefei 230036, Anhui Province, China
[b] Research Institute of Donkey High-Efficiency Breeding and Ecological Feeding, College of Agronomy, Liaocheng University, Liaocheng 252000, Shandong Province, China
[c] Biotechnology Center, Anhui Agricultural University, Hefei 230036, Anhui Province, China
[d] College of Animal Science and Technology, Nanjing Agricultural University, Nanjing 210095, Jiangsu Province, China

ARTICLE INFO

Article history:
Received 22 November 2023
Received in revised form
12 October 2024
Accepted 30 October 2024
Available online 7 November 2024

Keywords:
Undernutrition
Microbiota
Epithelial metabolism
Immune response

ABSTRACT

Nutrition consistently affects microbe-host interactions in the gastrointestinal tract. This study aimed to unravel how undernutrition reshapes the microbial composition and the homeostasis of epithelium in the jejunum and ileum. Sixteen late-gestation Hu-sheep were randomly assigned to the control group ($n = 8$, 100% ad libitum feeding levels) or the undernutrition group ($n = 8$, which received 30% ad libitum feeding levels). After 15-d treatment, all ewes were slaughtered, and jejunal and ileal digesta and epithelium samples were collected for 16S rRNA gene sequencing and transcriptome sequencing, respectively. Results indicated that undernutrition decreased the jejunal and ileal tissue weights ($P = 0.005$ and $P = 0.022$) and the levels of volatile fatty acids ($P = 0.019$ and $P = 0.007$) and microbial protein levels ($P = 0.019$ and $P = 0.031$) in jejunal and ileal digesta. The relative abundance of acetate producing microbiota, including *Clostridia UCG-014 norank*, *Ruminococcus*, *[Ruminococcus] gauvreauii*, and *Lachnospiraceae_Blautia*, were significantly reduced ($P < 0.05$) in the jejunum and ileum. Undernutrition up-regulated ($P < 0.05$) the expression of genes involved in amino acid synthesis and fatty acid oxidation, but down-regulated ($P < 0.05$) the expression of genes associated with amino acid degradation, fatty acid synthesis, and extracellular structures in jejunal and ileal epithelium. In the jejunal epithelium, genes associated with extracellular matrix–receptor interactions, cell growth, and immune response were down-regulated ($P < 0.05$) upon undernutrition. Taken together, undernutrition changed the microbial community in the jejunum and ileum, which altered the fermentation mode and the production of volatile fatty acids and microbial protein. These affected the energy and protein system in the epithelium and reprogrammed substance metabolism and extracellular structures, which probably further influenced cell growth and immune response. These insights provide a foundation for completely clarifying the crosstalk between small intestinal microbiota and the host.

1. Introduction

Small ruminants, particularly native breeds, play a significant role to the livelihoods of a considerable part of the local human population from socio-economic perspectives (Mohamadipoor Saadatabadi et al., 2021). Economical and biological efficiency of sheep production enterprises generally improves by increasing productivity and reproductive performance of ewes (Roudbar et al., 2018; Safaei et al., 2022). In ruminant production systems,

* Corresponding authors.
E-mail addresses: maoshengyong@njau.edu.cn (S. Mao), xueyanfeng@ahau.edu.cn (Y. Xue).
† These authors contributed equally to this work.
Peer review under the responsibility of Chinese Association of Animal Science and Veterinary Medicine.

Production and Hosting by Elsevier on behalf of KeAi

https://doi.org/10.1016/j.aninu.2024.10.004

physiological alteration can cause imbalances in the body's nutritional status, even when feed is adequately supplied (Chilliard et al., 1998). Sheep require more nutrients during late gestation because 80% of fetal weight is gained during this period (Rook, 2000). However, growing fetuses and expanding uterine size reduce abdomen and rumen size, leading to restricted feed intake (Cal Pereyra et al., 2012). As a result, ewes often experience an undernutrition in late pregnancy due to the conflict between higher nutritional requirements and lower nutritional intake, especially in multiple-bearing Hu-sheep. Undernutrition usually induces pregnancy toxemia, which threatens the health of pregnant ewes and inhibits fetal growth and development, resulting in weak or even stillborn lambs (Idamokoro et al., 2017; Ji et al., 2023; Kaiser, 1967). Researchers usually use very low feed intake, straw only feeding, or even complete starvation to construct the model of undernutrition or pregnancy toxemia (Bauer et al., 1995; Cal Pereyra et al., 2015; Fattet et al., 1984). In this study, we chose 30% of ad libitum feeding to establish an undernourished sheep model, which is closer to the physiological condition of Hu-sheep during late gestation.

The gastrointestinal tract plays a vital role in nutrient digestion, absorption and microbiota–host interactions which are important for the body's energy supply and metabolic homeostasis (Oliphant and Allen Vercoe, 2019; Rowland et al., 2018; Valdes et al., 2018). Disruptions of the microbiota–host interaction affect immune responses and metabolic homeostasis in the host (Dekaboruah et al., 2020; Neuman et al., 2015; Ogunrinola et al., 2020; Thaiss et al., 2016). Studies conducted on murine models revealed that acute undernutrition could lead to heightened levels of inflammation, which was attributable to changes in gut microbiota, compromised integrity of the gut barrier in the cecum and colon, and increased systemic exposure to lipopolysaccharide (Patterson et al., 2022). Previous study showed that undernutrition in ewes during late gestation altered microbial communities, epithelial substrate transport and metabolism, immune responses and microbiota–epithelium interaction in the rumen and large intestine (Wu et al., 2023; Xue et al., 2020a,b). The small intestine is an important site for nutrient digestion and absorption in animals (Judkins et al., 2020; Jung and Kim, 2022) and also provides a barrier against harmful substances such as pathogens, endotoxins, and antigens (Turner, 2009). In a mouse model, undernutrition was found to cause acute impairment of intestinal epithelial barrier integrity (Ribeiro et al., 2024). However, little is known about the effects of undernutrition during late pregnancy on small intestinal microbial–host interactions.

In this study, it was hypothesized that undernutrition during late gestation in sheep might affect the composition and function of the microbiota, fermentation in the jejunum and ileum, and subsequently, nutrient metabolism and immune response disruption in the jejunal and ileal epithelium. Therefore, this study aimed to investigate the response of jejunal and ileal microbiota and epithelium to undernutrition using 16S rRNA gene sequencing and transcriptome sequencing techniques.

2. Materials and methods

2.1. Animal ethics statement

All experimental procedures were conducted following the Animal Welfare Committee guidelines and the experimental protocol was approved (No. SYDW-P20190600601) by the Institutional Animal Care and Use Committee of Anhui Agricultural University, China. The procedures also met the ARRIVE guidelines (Kilkenny et al., 2010).

2.2. Experimental design and sample collection

This study formed part of a larger project which aimed to explore how undernutrition during late gestation affected the body's metabolic homeostasis (Liu et al., 2023). Briefly, 16 pregnant ewes (54.2 ± 2.75 kg, 108 d of gestation, 2–3 fetuses) were fed ad libitum for 7 d to calculate their feed intake. The diet formula and nutrient composition are detailed in Table 1. On the 115th d of gestation, the ewes were randomly divided into two groups: the control group (CON) ($n = 8$) was provided with 100% of the ad libitum feeding levels, and the undernutrition group (UN) ($n = 8$) was supplied with 30% of the ad libitum feeding levels. During the animal experiment, blood samples were collected every 5 d for the detection of β-Hydroxybutyrate (BHBA) and glucose levels. Results showed that, after 15-d feed restriction, blood BHBA level was higher than the threshold 0.8 mmol/L and blood glucose level was lower than the threshold 3 mmol/L, which indicated the successful establishment of an undernutrition model. On 130th day of gestation, all ewes were slaughtered at 4 h after their morning feeding, and jejunal and ileal epithelium and digesta samples were immediately collected and stored in liquid nitrogen for subsequent analysis.

2.3. Chemical analysis

In accordance with the established AOAC protocol (AOAC, 2016), the diet's nutritional components were determined, including: dry matter (method 930.15), crude protein (method 984.13), ether extract (method 2003.06), crude ash (method 942.05), neutral detergent fiber (method 2002.04), and acid detergent fiber (method 973.18). The concentrations of calcium and phosphorus (method 985.01) were quantified employing the technique of Inductively Coupled Plasma-Optical Emission Spectroscopy (ICP-OES) (AOAC, 2000). Metabolizable energy of the total mixed ration was calculated using the weighted method according to the metabolizable energy of each feed material in the China Feed Database and the proportion of the feed in the total mixed ration (Xiong et al., 2018).

Table 1
Ingredients and nutrient composition of the total mixed ration (%, dry matter basis).

Item	Content
Ingredient composition	
Whole corn silage	43.04
Peanut straw	31.07
Maize	17.79
Bean pulp	4.04
Soybean meal	2.70
Premix[1]	1.36
Total	100.00
Nutrient composition	
Metabolizable energy[2], MJ/kg	11.25
Crude protein	12.60
Ether extract	3.20
Neutral detergent fiber	40.19
Acid detergent fiber	34.20
Crude ash	5.23
Calcium	0.61
Phosphorus	0.31

[1] Provided the following per kilogram premix: vitamin A 150,000 IU, vitamin D_3 25,000 IU, vitamin E 1000 mg, Zn 2548 mg, Cu 370 mg, Fe 1500 mg, Mn 637 mg, I 35 mg, Se 11 mg, lysine 1.5%.
[2] The metabolizable energy was estimated.

2.4. Jejunal and ileal weight and morphological changes

After slaughtering, jejunal and ileal digesta were extracted from the intestinal lumen to measure the weight of emptied jejunal and ileal tissues. Fresh jejunal and ileal specimens were preserved in 4% paraformaldehyde for 24 h and subsequently stained with hematoxylin and eosin (H&E) to observe the epithelial morphology and quantify parameters including villus height, crypt depth, and the ratio of villus height to crypt depth (VH/CD).

2.5. Jejunal and ileal fermentation parameters

The pH of digesta samples from the jejunum and ileum was measured immediately after slaughtering with a pH meter HI 9125 (HANNA instrument, Woonsocket, RI, USA). The concentration of volatile fatty acids (VFAs) in the digesta samples were determined using a gas chromatography (GC-14B, Shimadzu, Japan). Digesta samples were homogenized in quadruple-distilled water and centrifuged at 2000 × *g* for 10 min. Subsequently, the supernatant was collected and mixed with 25% (w/v) metaphosphoric acid for VFA analysis (Qin, 1982). The capillary column of the gas chromatograph was 30 m × 0.32 mm × 0.25 μm with a column temperature of 130 °C, a vaporization temperature of 180 °C, and a detector temperature of 180 °C. The microbial protein (MCP) concentration of digesta samples were then determined by the Komas Brilliant Blue method (Bradford, 1976).

2.6. 16S rRNA gene sequencing analysis of microbiota in jejunal and ileal digests

DNA was extracted from the jejunal and ileal digesta samples using the bead beating and CTAB method (Zoetendal et al., 1998). The quality and concentration of each DNA sample were measured using a Nanodrop Spectrophotometer (Thermo, Madison, Wisconsin, USA). The V3–V4 region of the 16S rRNA gene was amplified (95 °C for 2 min, followed by 25 cycles at 95 °C for 30 s, 55 °C for 30 s, 72 °C for 30 s and a final extension at 72 °C for 5 min) using universal gene primers 341F (5′-CCTAYGGGRBGCASCAG-3′) and 806R (5′-GGACTACNNGGGTATCTAAT-3′). Amplicons (462 bp) were extracted from 2% agarose gels and purified using the QIAquick PCR Purification Kit (Qiagen, Hilden, Germany) and library construction was performed according to Illumina's instructions. The entire library was sequenced on the Illumina MiSeq PE-250 platform following standard protocol. Data were processed using the QIIME pipeline (v.1.9.0) and sequences were clustered into operational taxonomic units (OTUs) at a 97% sequence similarity level using UPARSE (v.7.1). The OTU representative sequences were classified using the RDP classifier (v.2.2) and compared to the SILVA database (v. 132). A total of 3695 and 4465 OTUs were identified in the jejunum and ileum, respectively.

2.7. Transcriptome assay of jejunal and ileal epithelium

Total RNA was extracted from jejunal and ileal epithelium using the Trizol method (Chomczynski and Sacchi, 1987). In order to ensure RNA quality, the absorption values of total RNA samples including A230, A260, and A280 were detected (both A260/230 and A260/280 were between 1.80 and 2.10) using a NanoDrop ND-1000 spectrophotometer (Thermo Scientific, Ilkirch, France) and the RNA integrity was confirmed by running 1.4% agarose-formaldehyde gel. Subsequently, a total of 10 RNA samples (5 from each group) were randomly selected for cDNA library construction. Firstly, mRNA was isolated from total RNA using the magnetic bead method. The first cDNA strand was synthesized using mRNA as a template, followed by the addition of buffer, dNTPs, RNase H and DNA polymerase I to synthesize the second cDNA strand, and finally the purified cDNA was ligated to the sequencing adapter. Suitable fragments (approximately 200–300 bps) were isolated using the NEBNext Ultra RNA Library Preparation Kit for PCR amplification. The cDNA library was constructed by selecting appropriate fragments and sequencing fragments on the Illumina Hi-Seq 2500 platform (Biomarker, Beijing, China). Clean reads were generated by removing low-quality reads and compared to the Sheep Reference Genome 4.0 using HiSAT2. The fragments per kilobase of transcript per million fragments mapped values (FPKMs) were calculated to show the expression of all genes. Differentially expressed genes (DEGs) were screened with the criteria of false-discovery rate (FDR) < 0.05 and fold change (FC) > 1.5 or < 0.667 using DESeq2 software (v.1.6.3). Volcano plots, clustering heatmaps, euKaryotic Orthologous Groups (KOG) functional classification, gene ontology (GO) enrichment analysis, gene set enrichment analysis (GSEA), and kyoto encyclopedia of genes and genomes (KEGG) pathway enrichment analysis were performed using a Biomarker platform (www.biocloud.net).

2.8. Real-time quantitative PCR analysis of genes in jejunal and ileal epithelium

The expression of target genes was measured by using a QuantStudio 5 real-time PCR instrument (Applied Biosystems, Foster, California, USA) and fluorescence detection of SYBR green dye, following the manufacturers' handbooks for Hieff qPCR SYBR Green Master Mix (Yeasen Biotechnology, Shanghai, China). The PCR mixture contained 2.0 μL of DNA template, 0.4 μL of forward primer (10 μmol/L), 0.4 μL of reverse primer (10 μmol/L), 10 μL of Hieff qPCR SYBR Green Master Mix (1*), and PCR-grade sterile water to a final volume of 20 μL. The program for PCR amplification was as follows: 95 °C for 5 min for pre-denaturation, and 40 cycles of 95 °C for 10 s, 60 °C for 30 s, followed by a melting curve program (60–99 °C with a ramping rate of 0.1 °C/s and fluorescence measurement). Gene expression data was normalized by the housekeeping gene (glyceraldehyde 3-phosphate dehydrogenase [*GAPDH*]) using the $2^{-\Delta\Delta Ct}$ method. Table S1 shows the primers for the genes.

2.9. Statistical analysis

An independent samples *t*-test in IBM SPSS 25.0 (IBM Corp, Armonk, New York, USA) was used to assess the significances of differences for tissue weights, fermentation parameters, epithelial morphology, and mRNA expressional levels of genes in the jejunum and ileum between CON and UN. Data were presented as means with their SEM. Microbial α-diversity and the relative abundance of bacteria in the jejunal and ileal digesta at the phylum and genus levels were statistically analyzed using a nonparametric test in IBM SPSS 25.0. $P < 0.05$ was used to determine statistical significance. Results were presented using GraphPad Prism 9 (GraphPad Software, Dotmatics, Boston, Massachusetts, USA). Spearman correlation coefficients (r) and the significance tests between fermentation parameters and microbiota were calculated using bivariate correlation ($n = 16$) in SPSS 25.0, and $P < 0.05$ was used to identify significant correlations. The *P*-values for enrichment significances of KEGG pathways were calculated using the clusterProfiler R package and corrected to obtain q values using multiple hypothesis testing. Power calculation showed that a required sample size of 8 ewes in each group could enable the detection of an effect size of 1.94 standard deviation (SD) for most of the cognitive test scores with 95% power and a type I error of 5%, based on the independent sample *t* test using the G*Power 3.1.9.4 Data Analysis (http://www.gpower.hhu.de/).

3. Results

3.1. Undernutrition affected jejunal and ileal morphology and fermentation mode

At the commencement of the experimental phase, the average body weight between CON and UN did not exhibit any significant difference ($P = 0.259$) (Table 2). However, following a 15-d treatment period, the body weight of ewes in UN was significantly diminished comparatively to CON ($P < 0.001$) (Table 2). UN showed significantly lower average daily weight gain than CON ($P < 0.001$) (Table 2). Undernutrition caused a significant decrease in weight of the empty jejunum ($P = 0.005$) and ileum ($P = 0.022$) and a significant increase in jejunal pH ($P = 0.022$) compared to CON (Table 3). According to H&E staining sections and morphological measurement analysis; jejunal villus height ($P = 0.025$) and VH/CD ($P = 0.006$) were lower while jejunal crypt depth ($P = 0.050$) and ileal crypt depth ($P = 0.017$) were higher in UN than those in CON (Table 3 and Fig. 1A and B). In jejunal and ileal digesta, the levels of acetate ($P = 0.011$ and $P = 0.007$), total VFAs ($P = 0.019$ and $P = 0.007$), and the molar ratio of acetate ($P = 0.002$ and $P = 0.003$) were significantly decreased, whereas the molar ratio of propionate ($P = 0.002$ and $P = 0.006$) was significantly increased in UN compared to CON (Table 3). Additionally, a significant increase was observed in the molar ratio of valerate ($P = 0.032$) in ileal digesta of UN. The levels of MCP ($P = 0.019$ and $P = 0.031$) in jejunal and ileal digesta were observed to be significantly decreased in UN as compared to CON (Table 3).

3.2. Undernutrition changed the diversity and composition of jejunal and ileal bacteria

To unravel the mechanisms behind the impacts of undernutrition on jejunal and ileal fermentation, we conducted 16S rRNA gene sequencing to investigate the changes in the bacterial communities within the jejunum and ileum. Rarefaction curves for all samples reached a plateau, indicating sufficient sequencing depth (Fig. S1A-B). The α-Diversity analysis showed that, compared to CON, Simpson's index increased ($P = 0.046$) in the jejunal digesta of UN, and Simpson's index ($P = 0.003$) increased while Shannon's ($P = 0.012$) and Evenness ($P = 0.006$) indexes decreased in the ileal digesta of UN (Fig. 1C). Principal-coordinate analysis (PCoA) based on Unweighted UniFrac metrics demonstrated the differences of the jejunal and ileal microbial community between CON and UN (Fig. 1D). In addition, the Venn diagrams revealed 564 and 1026 unique OTUs as well as 1337 and 784 unique OTUs in CON and UN for jejunal and ileal digesta, respectively (Fig. 1E).

Distinct characteristics were presented in the relative abundances of jejunal and ileal bacteria at the phylum and genus levels, with each taxon representing more than 0.5% in at least one group. In the jejunum, Firmicutes, Actinobacteriota, Patescibacteria, Unclassified, Proteobacteria, and *Bacteroidota* were the dominant phyla (relative abundance >1%) both in CON and UN. At the phylum level, the relative abundance of Firmicutes decreased ($P < 0.05$) in UN (Fig. 2A). In the ileum, Firmicutes, Actinobacteriota, Unclassified, Patescibacteria, and Bacteroidota were the dominant phyla (relative abundance >1%) in CON, while Proteobacteria and Verrucomicrobiota were the dominant phyla (relative abundance >1%) in UN. At the phylum level, the relative abundances of Unclassified and *Firmicutes* decreased ($P < 0.05$), while that of Proteobacteria increased ($P < 0.05$) in UN (Fig. 2B). At the genus level, the relative abundances of *Ruminococcus*, *Atopobiaceae_Olsenella*, *[Ruminococcus] gauvreauii group*, *Clostridia UCG-014_norank*, *Lachnospiraceae FE2018 group*, and *Lachnospiraceae_Blautia* increased ($P < 0.05$), while those of *Bifidobacteriaceae_Unclassified* and *Bifidobacteriaceae_Aeriscardovia* decreased ($P < 0.05$) in the jejunum of UN (Fig. 2C). Interestingly, the relative abundances of *Ruminococcus*, *Unclassified*, *Oscillospiraceae_NK4A214 group*, *Saccharofermentans*, *Clostridia UCG-014_norank*, *[Ruminococcus] gauvreauii group*, *Mycoplasma*, *Lachnospiraceae_uncultured*, *Ruminococcaceae_uncultured*, and *Lachnospiraceae_Blautia* in the ileum of UN decreased ($P < 0.05$) (Fig. 2D).

Table 2
Growth performance and daily feed intake of ewes in the CON and UN groups ($n = 8$).[1]

Item	Groups[2]		*P*-value
	CON	UN	
Initial body weight, kg	55.03 ± 1.073	53.43 ± 0.834	0.259
Final body weight, kg	56.80 ± 0.856[a]	44.06 ± 0.976[b]	<0.001
Daily weight gain, g/d	118.33 ± 35.495[a]	−624.17 ± 61.887[b]	<0.001
Daily feed intake, kg/d	1.63 ± 0.007[a]	0.52 ± 0.001[b]	<0.001

[a, b] Means in a row not sharing a common letter are significantly different ($P < 0.05$).
[1] The data are expressed as the mean ± SEM.
[2] CON, control group; UN, undernutrition group.

Table 3
Undernutrition affected the jejunal and ileal weight, morphology, and fermentation parameters ($n = 8$).[1]

Item	Groups[2]		*P*-value
	CON	UN	
Jejunum			
Emptied tissue weight, kg	0.96 ± 0.073[a]	0.71 ± 0.028[b]	0.005
pH	6.25 ± 0.114[b]	6.79 ± 0.174[a]	0.022
Villus height, μm	496.59 ± 26.842[a]	409.36 ± 22.058[b]	0.025
Crypt depth, μm	322.09 ± 36.706[b]	409.69 ± 17.804[a]	0.050
VH/CD	1.65 ± 0.170[a]	1.02 ± 0.093[b]	0.006
Acetate, mmol/L	4.60 ± 0.273[a]	3.72 ± 0.115[b]	0.011
Propionate, mmol/L	0.97 ± 0.015	1.03 ± 0.032	0.128
Butyrate, mmol/L	0.30 ± 0.045	0.22 ± 0.007	0.122
Valerate, mmol/L	0.12 ± 0.007	0.12 ± 0.006	0.827
Total VFAs, mmol/L	5.99 ± 0.318[a]	5.10 ± 0.114[b]	0.019
Acetate, %	76.61 ± 0.616[a]	72.99 ± 0.749[b]	0.002
Propionate, %	16.47 ± 0.665[b]	20.28 ± 0.787[a]	0.002
Butyrate, %	4.89 ± 0.535	4.39 ± 0.142	0.390
Valerate, %	2.03 ± 0.113	2.33 ± 0.128	0.098
MCP, mg/dL	64.26 ± 6.492[a]	42.58 ± 4.907[b]	0.019
Ileum			
Emptied tissue weight, kg	0.45 ± 0.064[a]	0.27 ± 0.031[b]	0.022
pH	7.36 ± 0.073	7.54 ± 0.059	0.073
Villus height, μm	493.27 ± 15.894	483.05 ± 38.423	0.809
Crypt depth, μm	201.38 ± 13.643[b]	272.50 ± 22.297[a]	0.017
VH/CD	2.55 ± 0.245	1.91 ± 0.299	0.120
Acetate, mmol/L	4.62 ± 0.329[a]	3.55 ± 0.090[b]	0.007
Propionate, mmol/L	0.89 ± 0.014	0.87 ± 0.003	0.175
Butyrate, mmol/L	0.24 ± 0.004	0.23 ± 0.009	0.268
Valerate, mmol/L	0.10 ± 0.010	0.13 ± 0.017	0.143
Total VFAs, mmol/L	5.85 ± 0.326[a]	4.78 ± 0.106[b]	0.007
Acetate, %	78.61 ± 1.161[a]	74.34 ± 0.367[b]	0.003
Propionate, %	15.50 ± 0.775[b]	18.25 ± 0.341[a]	0.006
Butyrate, %	4.18 ± 0.248	4.77 ± 0.190	0.082
Valerate, %	1.70 ± 0.229[b]	2.64 ± 0.323[a]	0.032
MCP, mg/dL	25.62 ± 3.284[a]	16.60 ± 1.853[b]	0.031

VFAs = volatile fatty acids; MCP = microbial protein; VH/CD = villus height to crypt depth.
[a, b] Means in a row not sharing a common letter are significantly different ($P < 0.05$).
[1] The data are expressed as the mean ± SEM.
[2] CON, control group; UN, undernutrition group.

3.3. Relationship between jejunal and ileal bacteria and fermentation parameters

This study investigated the correlation between shifts in bacterial genera and molar ratios of VFAs in both the jejunum and

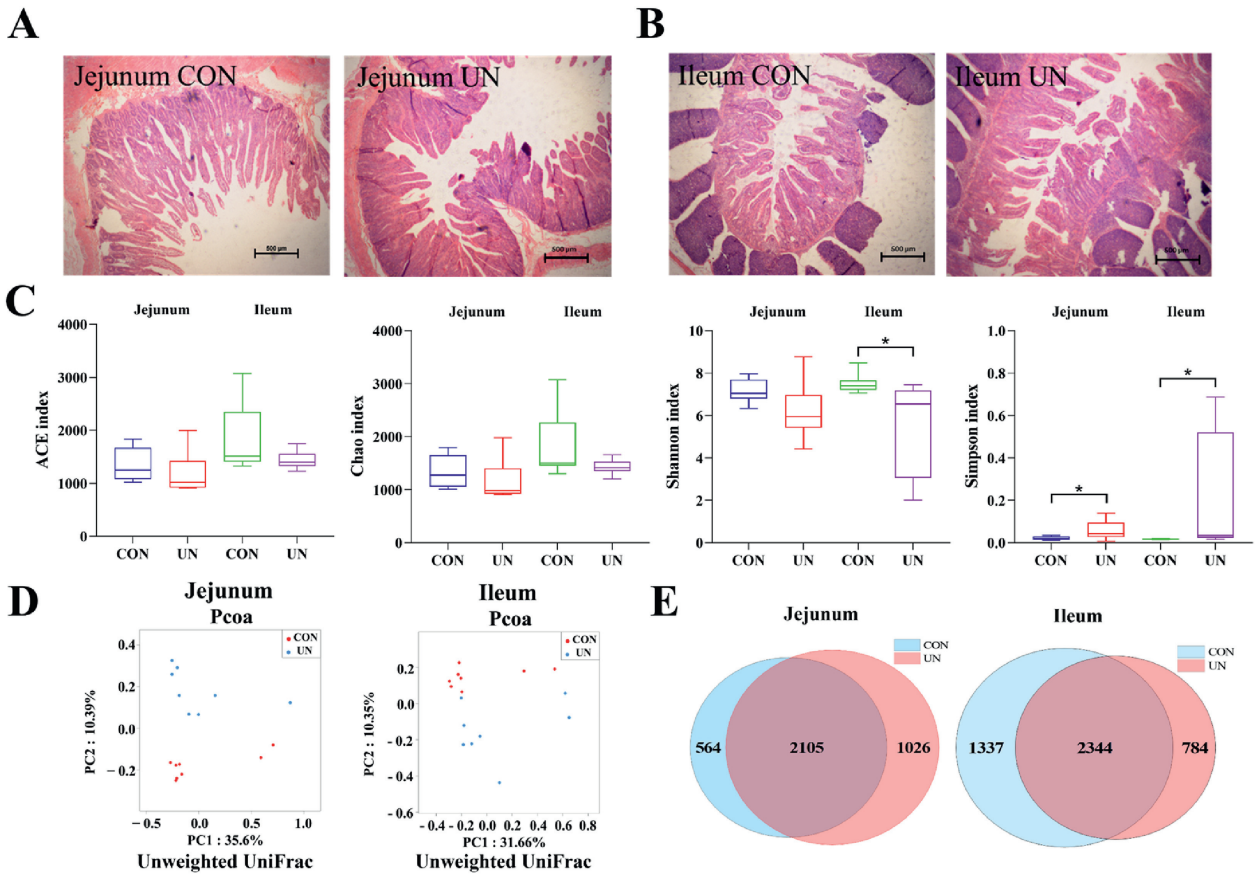

Fig. 1. Effect of undernutrition on the epithelial morphology and diversity of bacterial communities in jejunal and ileal digesta ($n = 8$). (A and B) Hematoxylin and eosin (H&E) stained sections and morphological measurements of jejunal and ileal epithelium. (C) Jejunal and ileal α diversity. (D) PCoA of bacterial communities based on OTUs in jejunal and ileal digesta. (E) Venn diagram of OTUs in jejunal and ileal digesta. Asterisks indicate significant differences ($P < 0.05$). CON, control group; UN, undernutrition group. PCoA = principal-coordinate analysis; OTUs = operational taxonomic units.*, $P < 0.05$.

ileum, exploring the relationship between microbiota and fermentation parameters. In the jejunum, the relative abundance of *Clostridia UCG-014_norank*, Lachnospiraceae *FE2018 group*, *Ruminococcus, [Ruminococcus] gauvreauii group*, and *Lachnospiraceae_Blautia* correlated positively with that of acetate and negatively with the molar ratio of propionate. The molar ratio of acetate was also negatively correlated with the relative abundance of *Bifidobacteriaceae_Aeriscardovia* and *Bifidobacteriaceae_Unclassified*. The molar ratio of propionate was positively correlated with the relative abundance of *Bifidobacteriaceae_Aeriscardovia* and negatively with the relative abundance of *Atopobiaceae_Olsenella*. The molar ratio of valerate was positively correlated with the relative abundance of *Bifidobacteriaceae_Unclassified* and negatively correlated with that of *Clostridia UCG-014_norank* (Fig. 3A). In the ileum, the molar ratio of acetate was positively correlated with the relative abundance of *Clostridia UCG-014_norank*, *Ruminococcus*, *[Ruminococcus] gauvreauii group*, *Lachnospiraceae_Blautia*, *Ruminococcaceae_uncultured*, *Mycoplasma*, and *Unclassified*. The molar ratio of propionate was positively correlated with the relative abundance of *Clostridia UCG-014_norank*, *Ruminococcus*, *[Ruminococcus] gauvreauii group*, *Lachnospiraceae_Blautia*, and *Ruminococcaceae_uncultured*. The molar ratio of valerate was negatively correlated with *Clostridia UCG-014_norank*, *Ruminococcus*, *[Ruminococcus] gauvreauii group*, Lachnospiraceae_*Blautia*, *Unclassified*, and *Saccharofermentans* (Fig. 3B). Interestingly, none of the significantly altered genera in the jejunum and ileum exhibited a strong correlation with the molar ratio of butyrate. Functional classification of bacteria in the jejunum and ileum were completed using the KEGG database at level II. Results showed that xenobiotic biodegradation and metabolism, metabolism of terpenoids and polyketides, metabolism of other amino acids, biosynthesis of other secondary metabolites, and cell growth and death were enhanced ($P < 0.05$), while transcription was weakened ($P < 0.05$), in the jejunum of UN (Fig. 3C). Metabolism, xenobiotic biodegradation and metabolism, and metabolism of other amino acids were enhanced ($P < 0.05$), while carbohydrate metabolism, replication and repair, translation, and transcription were weakened ($P < 0.05$) in the ileum of UN (Fig. 3D).

3.4. Undernutrition altered the transcriptional profile of jejunal and ileal epithelium

Given the interaction between microbiota and host, transcriptome sequencing of epithelial samples was conducted to explore the effect of undernutrition on substance transport and metabolism, and cellular structures and functions, in the epithelium of jejunum and ileum. Volcano maps showed that a total of 291 and 138 DEGs were identified between the two groups in the jejunal and ileal epithelium, respectively (Fig. S2A-B). Seventy-three DEGs were up-regulated and 218 DEGs were down-regulated in the jejunum of UN while 40 DEGs were up-regulated and 98 DEGs were down-regulated in the ileum of UN as compared to CON. Clustering heatmaps of the DEGs in the jejunal and ileal epithelium both showed that samples from CON and UN were grouped into two distinct classes (Fig. S3A-B). Principal component analysis (PCA) and partial least squares discriminant analysis (PLS-DA) plots revealed substantial disparities in total

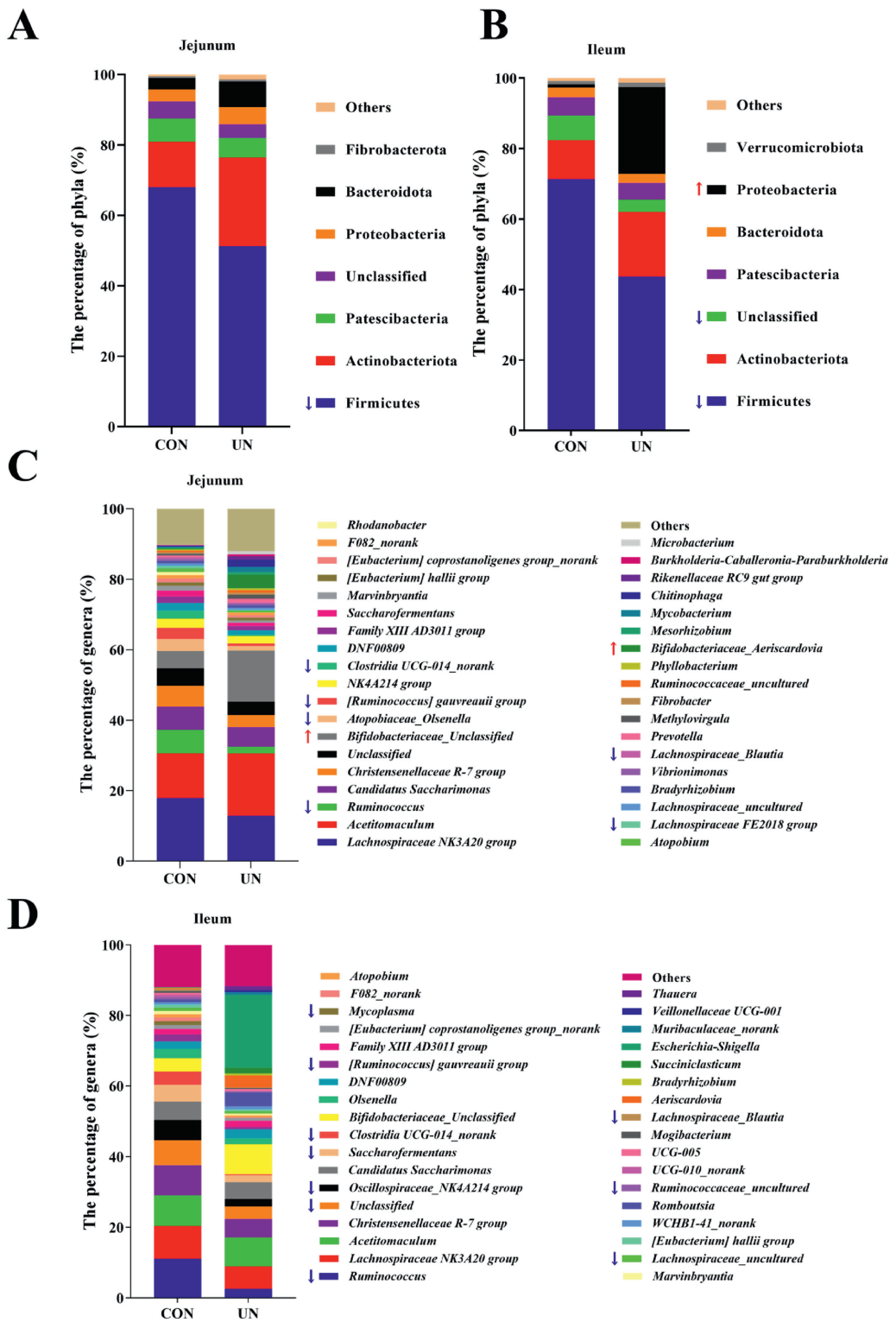

Fig. 2. Undernutrition changed the structures of bacterial communities in jejunal and ileal digesta ($n = 8$). (A and B) Relative abundance of bacterial communities at the phylum level in jejunum and ileum. (C and D) Relative abundances of bacterial communities at the genus level in jejunum and ileum. Red arrows indicate significant increases ($P < 0.05$) and blue arrows indicate significant decreases ($P < 0.05$) of abundances distributed in the pointed biological process. CON, control group; UN, undernutrition group.

transcriptome profiles between CON and UN; both in the jejunum and ileum (Fig. 4A–D). To further elucidate the function of DEGs between CON and UN, functional classification was conducted using KOG. Results showed that amino acid transport and metabolism, lipid transport and metabolism, and extracellular structures were enriched by DEGs in the jejunum and ileum (Fig. 5A and B), in addition to the general function prediction and signal transduction mechanisms. KEGG pathway enrichment analysis showed advanced glycosylation end (AGE) signaling pathway in diabetic complications, phosphoinositide 3 kinase-protein kinase B (PI3K-

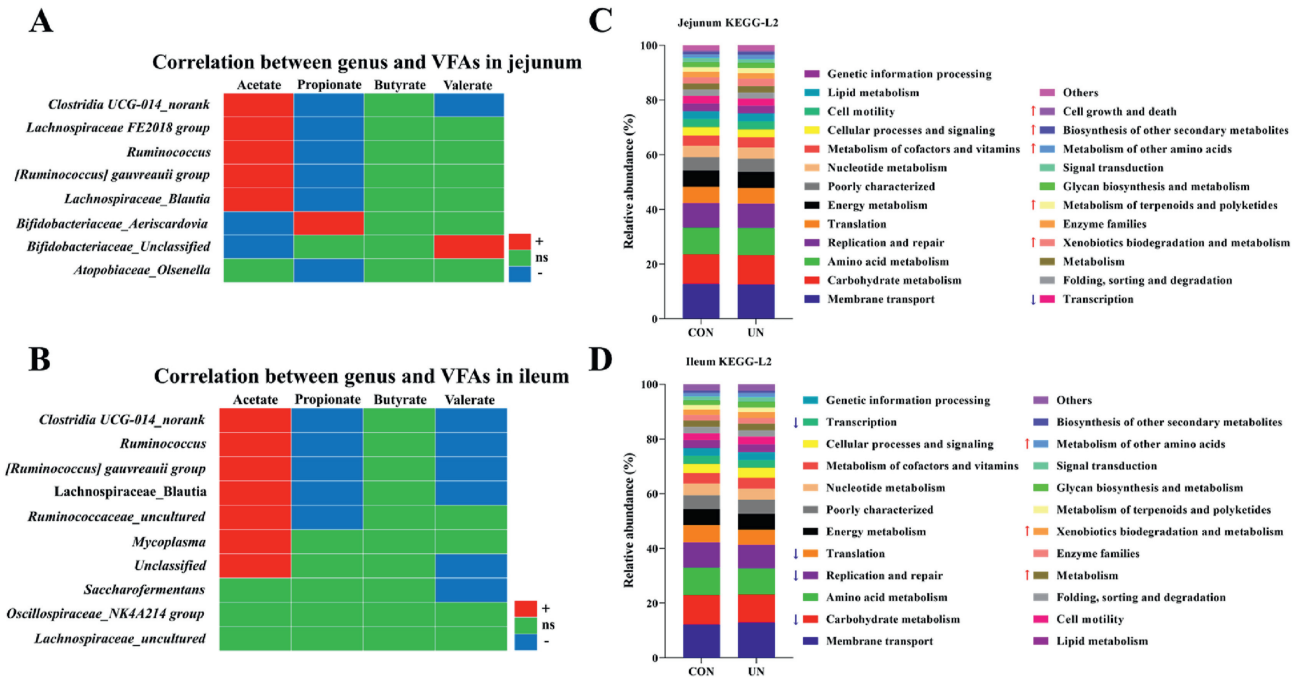

Fig. 3. Undernutrition changed the correlation of bacterial and fermentation parameters and bacterial KEGG function in jejunal and ileal digesta ($n = 8$). (A and B) Correlations between the changed bacterial communities and fermentation parameters in the jejunal and ileal digesta. (C and D) Abundance distribution map of jejunal and ileal microbiota based on KEGG prediction function. "+" indicates a significant positive correlation ($P < 0.05$), "-" indicates a significant negative correlation ($P < 0.05$), and "ns" indicates a nonsignificant correlation ($P > 0.05$). Red arrows indicate significant increases ($P < 0.05$) and blue arrows indicate significant decreases ($P < 0.05$) of abundances distributed in the pointed biological process. CON, control group; UN, undernutrition group. KEGG = kyoto encyclopedia of genes and genomes.

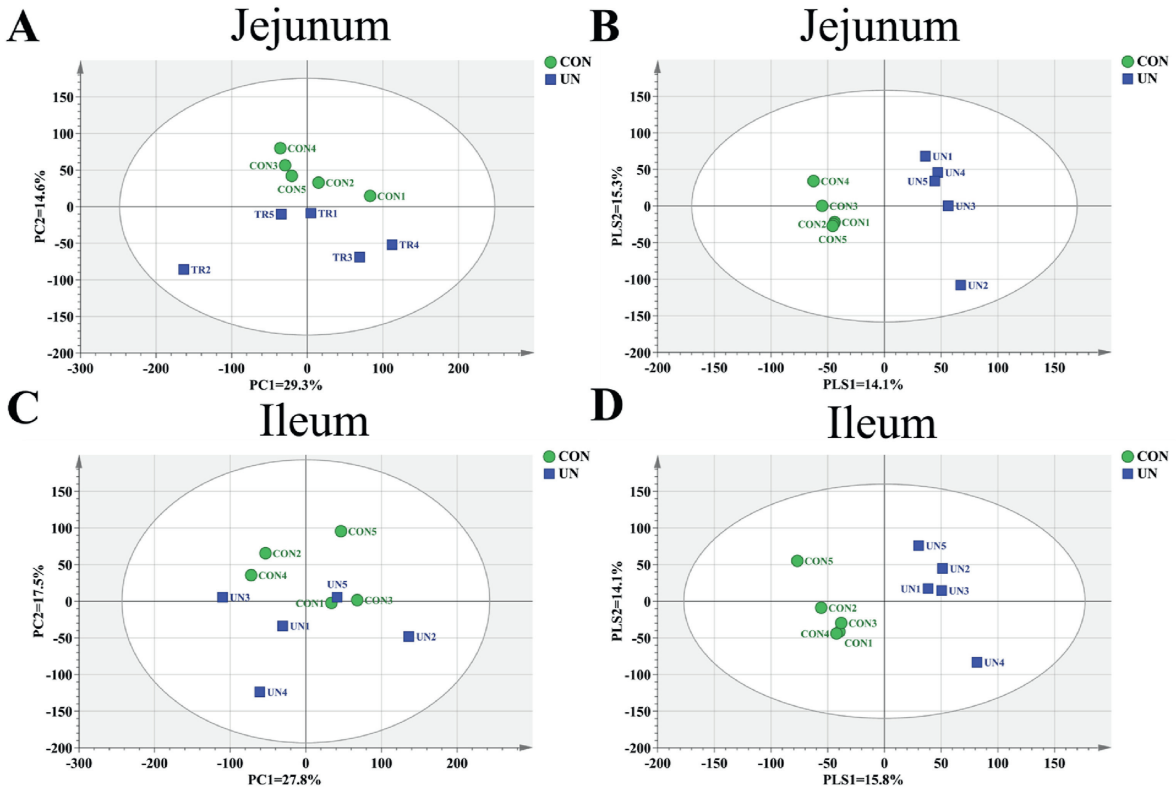

Fig. 4. The PCA and PLS-DA of total genes in the jejunal and ileal epithelium of ewes in CON and UN ($n = 5$). (A and B) PCA and PLS-DA of total genes in the jejunal epithelium. (C and D) PCA and PLS-DA of total genes in the ileal epithelium. CON, control group; UN, undernutrition group. PCA = principal component analysis; PLS-DA = partial least squares discriminant analysis.

Akt) signaling pathway, and peroxisome proliferator-activated receptor (PPAR) signaling pathway were enriched in the jejunum ($q < 0.05$), while only the PPAR signaling pathway was enriched in the ileum ($q < 0.05$) (Fig. 5C and D).

3.5. Undernutrition reprogrammed substance metabolism in jejunal and ileal epithelium

Transcriptome results revealed that DEGs associated with amino acid synthesis, including *phgdh*, *psat1*, *asns*, and *gpt2* were up-regulated in the jejunum of UN group compared to the CON group (Fig. 6A). In contrast, DEGs associated with peptidases (*c1r*, *c1s*, *mcp1*, *pamr1*, *tpsb2*, *masp1*, and *kel*) and amino acid degradation (*aass* and *hdc*) were all down-regulated. Differentially expressed genes associated with amino acid synthesis (*gpt2*, *psph*, *psat1*, and *asns*) and amino acid transport (*slc1a5* and *slc7a5*) were up-regulated in the ileal UN (Fig. 6B). Overall, amino acid synthesis and transport were enhanced while amino acid degradation, peptidases, collagen, cell adhesion, and extracellular matrix (ECM) metabolism were inhibited in jejunal and ileal epithelium of undernourished ewes.

Lipids play a pivotal role in providing energy to the body and are regulated by PPAR signaling pathway (Bougarne et al., 2018; Da Poian et al., 2010). Gene set enrichment analysis was performed on jejunal and ileal DEGs, which are associated with the enrichment of the PPAR pathway (Fig. 6C and D). And the transcriptome results indicated that DEGs associated with fatty acid oxidation (*cpt1a*, *cpt1b*, *cpt2*, *acadvl*, *acaa2*, and *hmgcs2*) and adipocyte differentiation (*plin2* and *fabp4*) were up-regulated in UN in jejunal lipid metabolism (Fig. 6E–G). Conversely, DEGs related to fatty acid synthesis (*fads1*, *fads2*, and *plpp3*) and retinoic acid degradation (*cyp26b1*) were down-regulated. Differentially expressed genes associated with fatty acid transport, such as *rbp1* and *abca6*, were down-regulated, while *fabp4* and *fabp5* were up-regulated. Ileal lipid metabolism showed similar results to that of the jejunum, although there was a significant reduction in enriched DEGs

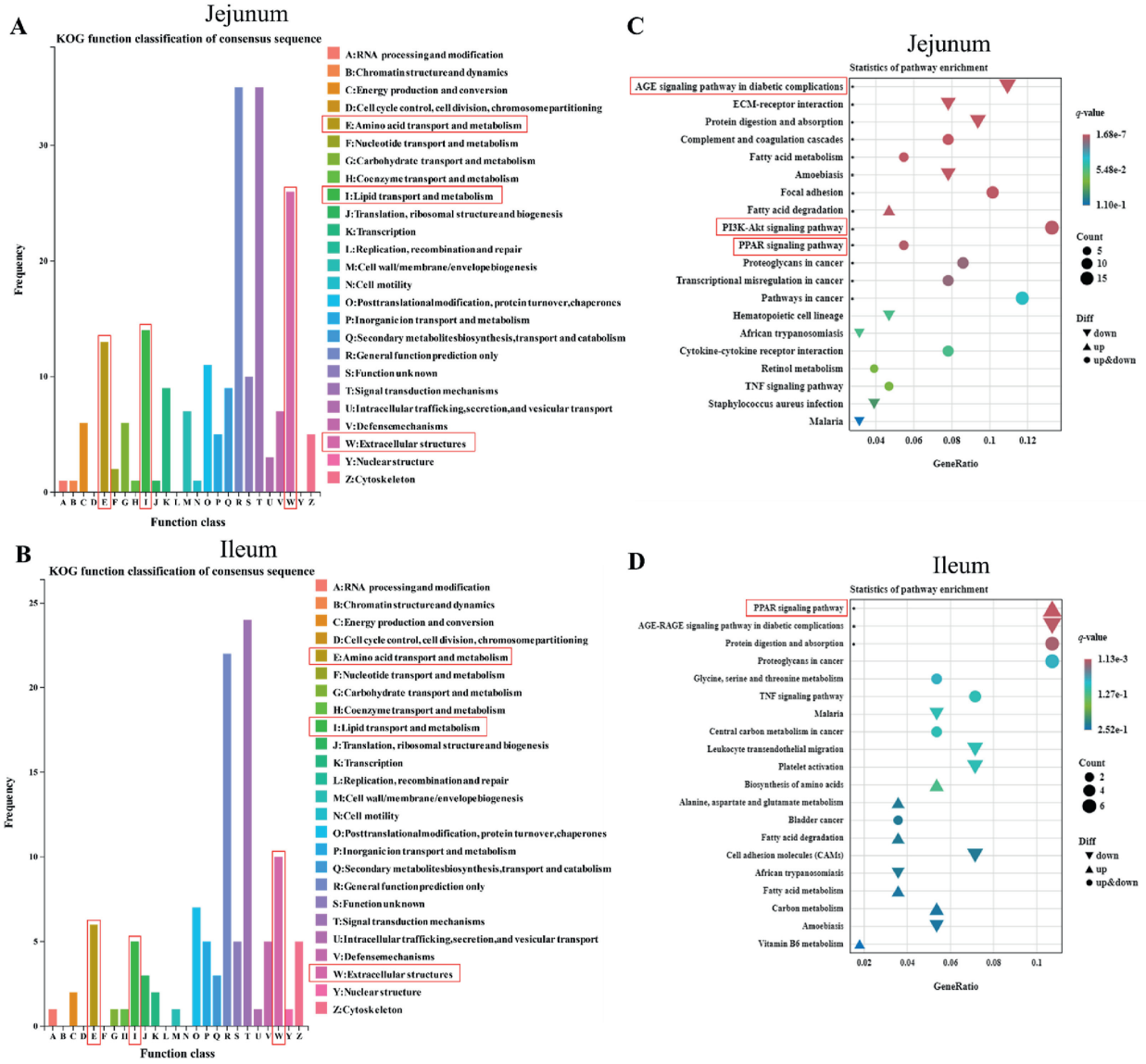

Fig. 5. Effect of undernutrition on the transcriptome profiles of jejunal and ileal epithelium ($n = 5$). (A and B) KOG function classification of DEGs in the jejunal and ileal epithelium. (C and D) KEGG pathway enrichment analysis of DEGs in jejunum and ileum. The X-axis indicates the function classification of KOG and the Y-axis indicates the number of DEGs. Asterisks indicate the significantly enriched pathways ($q < 0.05$). CON, control group; UN, undernutrition group. KOG = euKaryotic orthologous groups; KEGG = kyoto encyclopedia of genes and genomes; DEGs = differentially expressed genes.

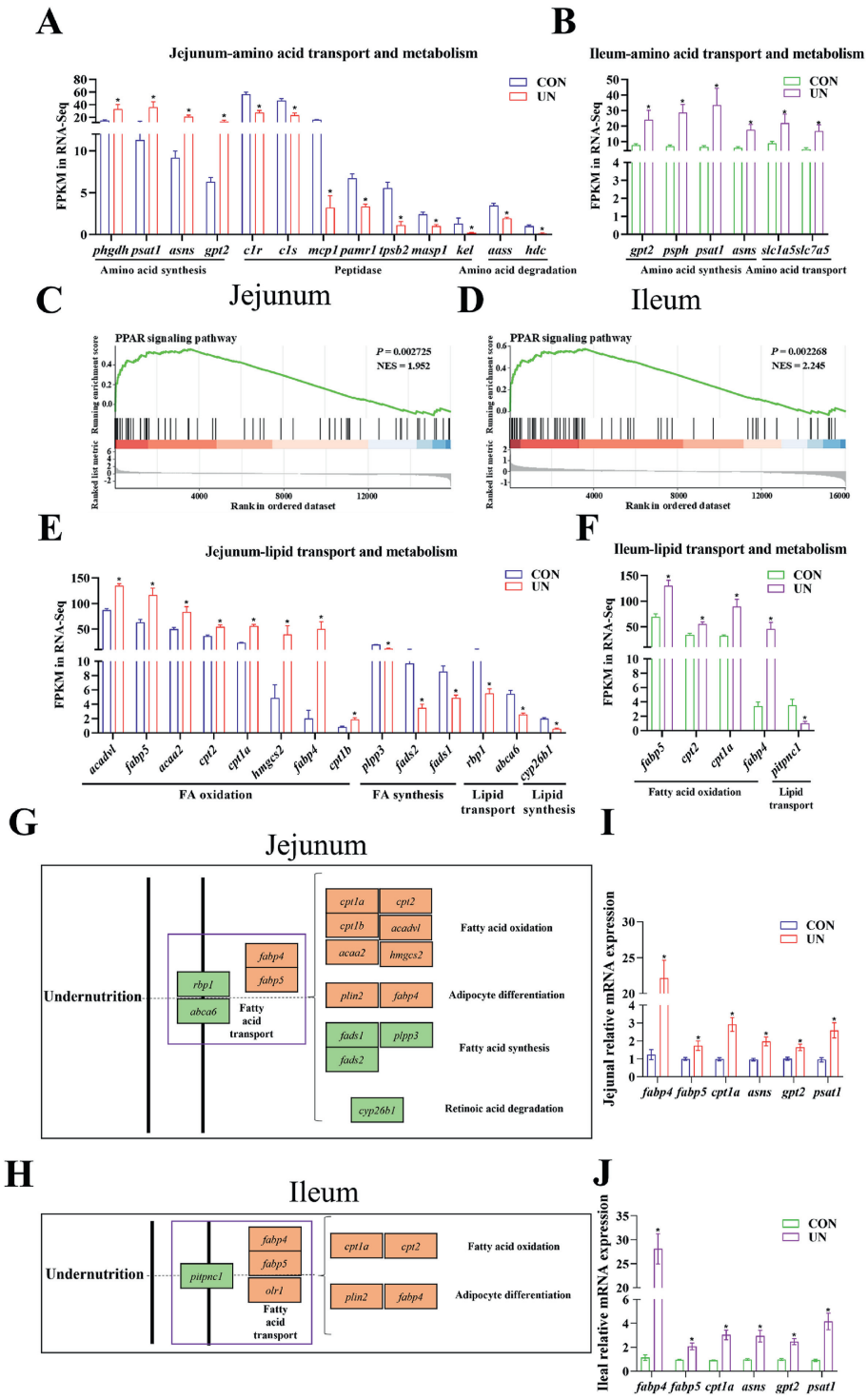

Fig. 6. Undernutrition reprogrammed substance metabolism of the jejunal and ileal epithelium. (A and B) Expression of genes related to amino acid transport and metabolism in jejunal and ileal epithelium ($n = 5$). (C and D) GSEA map of PPAR signaling pathways in jejunal epithelium ($n = 5$). (E and F) Expression of genes related to lipid transport and metabolism in jejunal and ileal epithelium ($n = 5$). (G and H) Schematic diagram of signaling involved in the PPAR pathway in jejunal and ileal epithelium ($n = 5$). (I and J) Real-time quantitative PCR of jejunal and ileal epithelium ($n = 8$). Asterisks indicate significant differences ($P < 0.05$). Red background indicates up-regulated DEGs while green background indicates down-regulated DEGs. CON, control group; UN, undernutrition group. GSEA = gene set enrichment analysis; NES = normalized enrichment score; PPAR = peroxisome proliferator-activated receptor; DEGs = differentially expressed genes. *phgdh* = phosphoglycerate dehydrogenase; *psat1* = phosphoserine aminotransferase 1; *asns* = asparagine synthetase; *gpt2* = glutamic-pyruvic transaminase 2; *c1r* = complement c1r; *mcp1* = c–c motif chemokine ligand 2; *pamr1* = peptidase domain containing associated with muscle regeneration 1; *tpsb2* = tryptase beta 2; *masp1* = mbl associated serine protease 1; *kel* = kell metallo-endopeptidase; *aass* = aminoadipate-semialdehyde synthase; *hdc* = histidine decarboxylase; *psph* = phosphoserine phosphatase; *slc1a5* = solute carrier family 1 member 5; *acadvl* = acyl-coa dehydrogenase very long chain; *fabp5* = fatty acid binding protein 5; *acaa2* = acetyl-coa acyltransferase 2; *cpt2* = carnitine palmitoyltransferase 2; *hmgcs2* = 3-hydroxy-3-methylglutaryl-coa synthase 2; *cpt1b* = carnitine palmitoyltransferase 1b; *plpp3* = phospholipid phosphatase 3; *fads2* = fatty acid desaturase 2; *rbp1* = retinol binding protein 1; *abca6* = atp binding cassette subfamily a member 6; *cyp26b1* = cytochrome p450 family 26 subfamily b member 1; *pitpnc1* = phosphatidylinositol transfer protein cytoplasmic 1; *plin2* = perilipin 2; *olr1* = oxidized low density lipoprotein receptor 1.*, $P < 0.05$.

(Fig. 6F–H). Differentially expressed genes linked to fatty acid oxidation (*cpt1a* and *cpt2*) and adipocyte differentiation (*plin2* and *fabp4*) were also up-regulated. Differentially expressed genes associated with fatty acid transport, such as *pitpnc1*, were down-regulated, while *fabp4*, *fabp5*, and *olr1* were up-regulated. A study showed that fasting also led to enhanced fatty acid oxidation in mice (Zhang et al., 2024). Considering the significant influence of undernutrition on amino acid and lipid metabolism, real-time quantitative PCR was used to examine several relevant genes. As expected, *fabp4*, *fabp5*, *cpt1a*, *asns*, *gpt2*, and *psat1* were up-regulated in UN (Fig. 6I and J). In conclusion, undernutrition modulated fatty acid metabolism, adipocyte differentiation and retinol degradation in the jejunal and ileal epithelium.

3.6. Undernutrition-inhibited cellular structures and functions in jejunal and ileal epithelium

The jejunum transcriptome results revealed extracellular structures, particularly highlighting that DEGs linked with collagen (*col1a1*, *col1a2*, *col3a1*, *col4a4*, *col4a5*, *col4a6*, *col5a1*, *col5a2*, *col6a1*, *col6a2*, *col11a2*, and *col27a1*), cellular adhesion (*postn*, *lama4*, *olfml3*, *olfml1*, *nid1*, *nid2*, *itga9*, and *ctnnd2*), ECM synthesis (*sparc*), ECM degradation (*mmp3*, *mmp9*, and *mmp19*), and cellular migration (*slit3*) were all down-regulated in the UN (Fig. 7A). Differentially expressed genes associated with collagen (*col1a1*, *col1a2*, *col3a1*, *col5a2*, and *col5a1*), cell adhesion (*postn* and *olfml1*), ECM synthesis (*sparc*), ECM degradation (*mmp9*), and cellular migration (*slit3*) exhibited down-regulation in the ileal UN (Fig. 7B). In mouse models, protein undernutrition was thought to impair collagen synthesis (Seth et al., 2024). Due to the significant impact of undernutrition on extracellular structures, real-time quantitative PCR was used to analyze several relevant genes. As expected, significant down-regulation was observed in *col1a1*, *col1a2*, and *col3a1* in UN (Fig. 7C and D).

GSEA conducted on jejunal DEGs confirmed the enrichment of the PI3K-AKT and AGE-RAGE pathways (Fig. 7E and F). Differentially expressed genes involved in ECM (*col1a1*, *col1a2*, *col4a4*, *col4a5*, *col4a6*, *col6a1*, *col6a2*, *fn1*, and *lama4*) and growth factor (*vegfc*, *kitlg*, and *pdgfb*), cellular membrane receptors (*igha1* and *gnb4*), and downstream biological processes involved in cell growth (*serpine1* and *vegfc*) and immune response (*ccl2*, *serpine1*, *vcam1*, and *f3*) were all down-regulated (Fig. 7G). This study suggested that undernutrition disrupted the production of upstream ECM and growth factor, and impeded their interactions with cell membrane receptors.

4. Discussion

During late gestation, the rapid intrauterine growth and development of the fetus; particularly in cases of multiple fetuses, significantly increased nutritional demand, leading to disparity between nutritional supply and nutritional consumption. Despite its critical significance, there is a notable lack of data demonstrating how undernutrition affects the small intestinal microbiota and epithelium in pregnant ewes. Our results demonstrated that VFA and MCP levels were decreased, both in jejunal and ileal digesta during undernutrition, which is highly consistent with the decreased concentrations of VFAs and MCP observed in ruminal digesta of pregnant ewes during undernutrition (Xue et al., 2020b). This finding possibly resulted from the dearth of available fermentable substrates in the rumen and small intestine upon undernutrition. Additionally, this study showed significant alterations in the molar ratios of acetate, propionate, and valerate in jejunal and ileal digesta during undernutrition. Essentially, the shift in the molar ratio of VFAs was attributed to the modification in the structure of microbial community (Felizardo et al., 2019). In previous studies, it was demonstrated that the genus *Clostridia UCG-014 norank* exhibited a positive correlation with acetate molar ratio (Wu et al., 2023). Additionally, *Ruminococcus* was identified as an essential component of carbohydrate-active enzymes that facilitated the production of acetate from transient glucose generated during the degradation of maltose oligosaccharides and starch (Crost et al., 2018), and *[Ruminococcus] gauvreauii* utilizes formate to produce acetate through the Wood Ljungdahl pathway (Molinero et al., 2022). *Lachnospiraceae_Blautia* was capable of producing acetate from the end products of glucose metabolism (San Juan Vergara et al., 2018). *Ruminococcaceae_uncultured* positively correlated with acetate molar ratios and negatively with propionate molar ratios (Lv et al., 2020). In the current study, the correlations between altered microbial genera and VFA molar ratios were highly consistent with those described in the references mentioned above. Consequently, the observed decrease in acetate molar ratio in the jejunum and ileum could be attributed to the decreased relative abundance of *Clostridia UCG-014 norank*, *Ruminococcus*, *[Ruminococcus] gauvreauii*, and *Lachnospiraceae_Blautia*. Conversely, the increase in propionate molar ratio in the ileum may be due to the decreased relative abundance of *Ruminococcaceae_uncultured*. In summary, this study revealed that undernutrition could affect the microbial community within the digesta of the jejunum and ileum during late pregnancy which might result in alterations molar ratios of VFAs. Furthermore, total VFAs and MCP were significantly lowered due to reduced feed intake.

Undernutrition could imbalance the microbial diversity that leads the decreased production of MCP and VFAs by the microbiota of ilea and jejunum, which may significantly affect the metabolism of epithelial substrates. Resultantly, DEGs were significantly enriched in the KOG functional classification for the metabolism of amino acids, lipids, and ECM. Notably, the analysis revealed a greater enrichment of DEGs relevant to these metabolic pathways in the jejunum (53 DEGs) compared to the ileum (21 DEGs). Humans and pigs were also deficient in a variety of amino acids such as valine, methionine, phenylalanine, and threonine during undernutrition (Jiang et al., 2016; Smith et al., 1974). Microbial protein represented a major source of amino acids for ruminants (Pathak, 2008); thus, the elevated amino acid synthesis and transport and the repressed amino acid degradation in the epithelium may have been attributed to reduced levels of intestinal MCP. Furthermore, the down-regulated expression of genes associated with ECM in the jejunum and ileum may also attribute to the reduction of MCP levels. As VFAs generated by gut microbial fermentation constituted a major source of energy for ruminants (Bergman, 1990; Penner, 2014), lower concentrations of VFAs suggested a dearth of available energy for undernourished ewes. Interestingly, in the PPAR signaling pathway, the enhanced fatty acid oxidation in the jejunal and ileal epithelium indicated an increase in energy availability to the host, while the suppressed fatty acid synthesis, steroid synthesis, and lipid transport implied a reduction in energy expenditure by the host. These metabolic changes in the jejunal and ileal epithelium upon undernutrition were similar with the consequences of ruminal and cecal epithelium in undernourished pregnant ewes reported in previous studies, exhibiting enhanced energy production and reduced energy consumption (Wu et al., 2023; Xue et al., 2020b). Taken together, these findings suggested that, in order to adapt the low VFA and MCP levels generated from microbiota fermentation upon undernutrition, pregnant ewes adjusted substrate transport and metabolism in the epithelium to elevate the utilization efficiency of amino acids and to increase energy production and decrease energy expenditure.

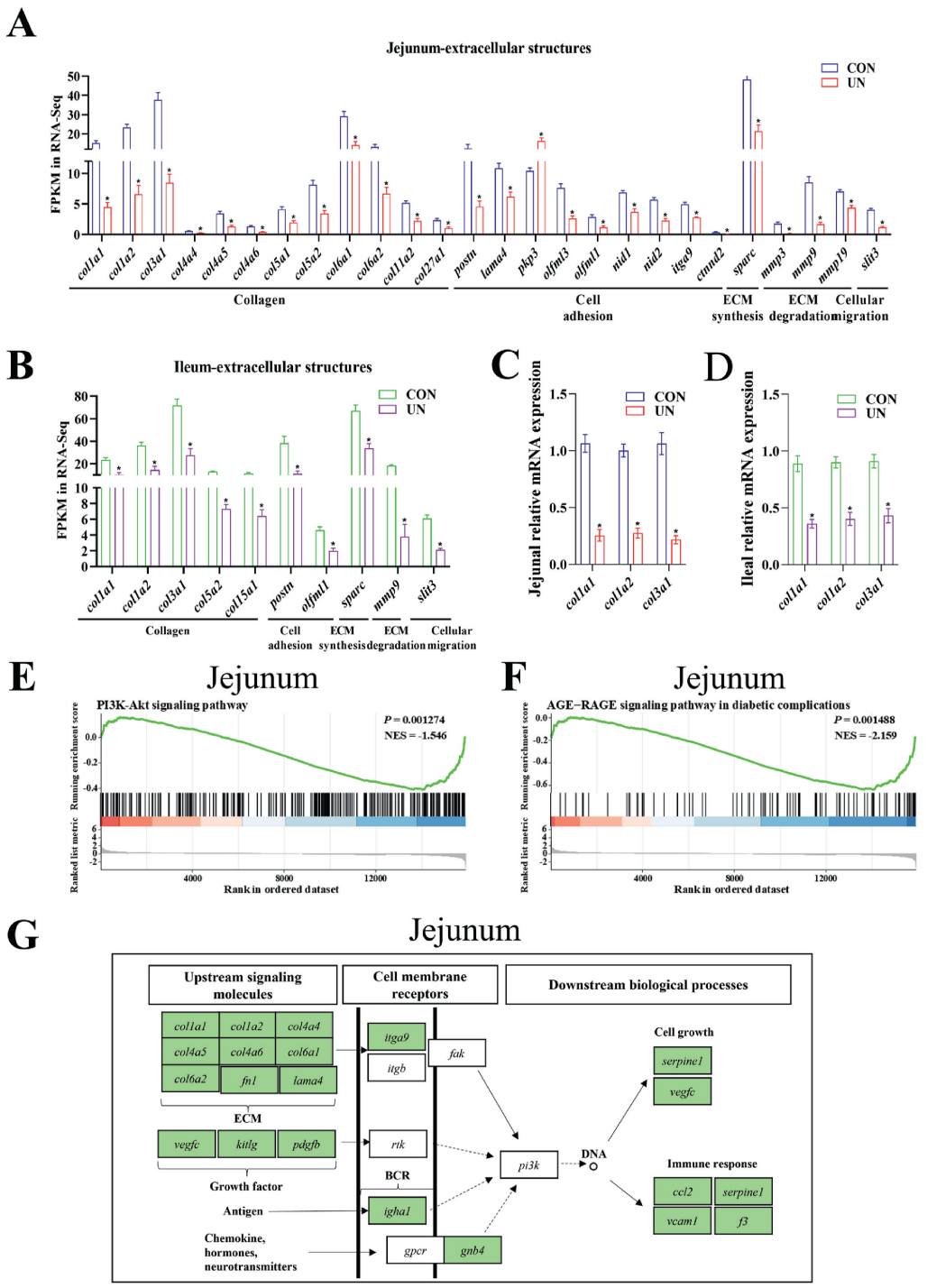

Fig. 7. Undernutrition inhibitory cell growth and immune response in jejunal and ileal epithelium. (A and B) Expression of genes related to extracellular structures in jejunal and ileal epithelium (n = 5). (C and D) Real-time quantitative PCR of jejunal and ileal epithelium (n = 8). (E and F) Gene set enrichment analysis map of PI3K-AKT and AGE-RAGE signaling pathways in jejunal epithelium (n = 5). (G) Schematic diagram of signaling involved in the PI3K-AKT and AGE-RAGE pathways in jejunal epithelium (n = 5). Asterisks indicate significant differences (P < 0.05). Red background indicates up-regulated DEGs while green background indicates down-regulated DEGs. CON, control group; UN, undernutrition group. ECM = extracellular matrix; GSEA = gene set enrichment analysis; NES = normalized enrichment score; PI3K-AKT = phosphoinositide 3 kinase-protein kinase B; DEGs = differentially expressed genes; BCR=B-cell receptor; *col1a1* = collagen type i alpha 1 chain; *postn* = periostin; *lama4* = laminin subunit alpha 4; *pkp3* = plakophilin 3; *olfml3* = olfactomedin like 3; *nid1* = nidogen 1; *itga9* = integrin subunit alpha 9; *ctnnd2* = catenin delta 2; *sparc* = secreted protein acidic and cysteine rich; *mmp3* = matrix metallopeptidase 3; *slit3* = slit guidance ligand 3; *fn1* = fibronectin 1; *vegfc* = vascular endothelial growth factor c; *kitlg* = kit ligand; *pdgfb* = platelet derived growth factor subunit b; *igha1* = immunoglobulin heavy constant alpha 1; *gnb4* = g protein subunit beta 4; *serpine1* = serpin family e member 1; *ccl2* = c−c motif chemokine ligand 2; *vcam1* = vascular cell adhesion molecule 1; *f3* = coagulation factor iii, tissue factor. *, P < 0.05.

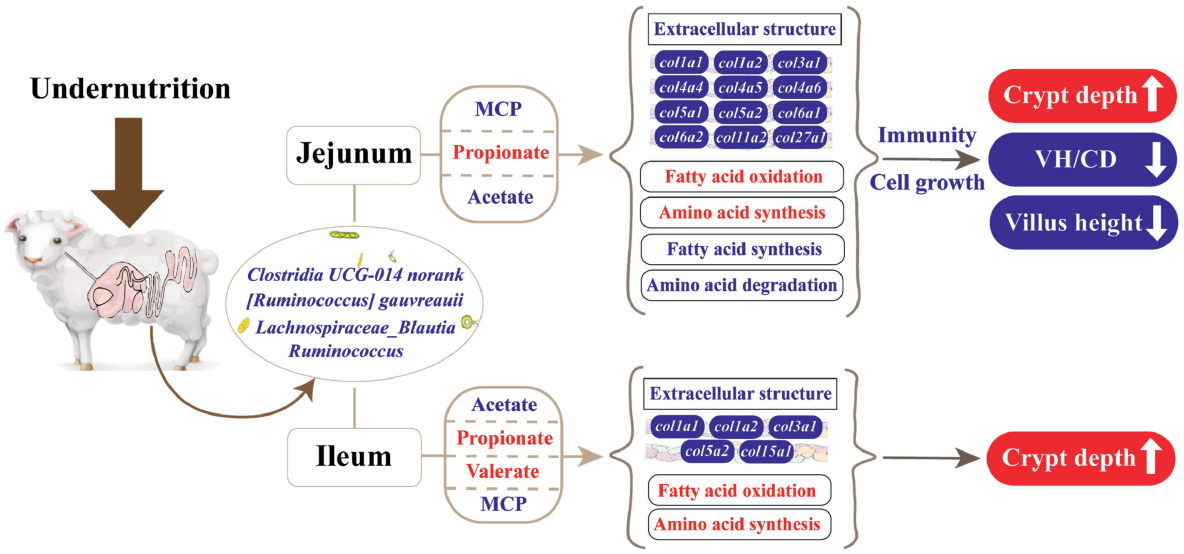

Fig. 8. Disruptions of jejunal and ileal microbiota and epithelial homeostasis upon undernutrition. +, positive correlation; −, negative correlation. Red or blue background and font represent up-regulated or down-regulated microbiota, genes, metabolites, and biological processes in undernourished ewes, respectively. MCP = microbial protein; *col1a1* = collagen type i alpha 1 chain; *col1a2* = collagen type i alpha 2 chain; *col3a1* = collagen type iii alpha 1 chain; *col4a4* = collagen type iv alpha 4 chain; *col4a5* = collagen type iv alpha 5 chain; *col4a6* = collagen type iv alpha 6 chain; *col5a1* = collagen type v alpha 1 chain; *col5a2* = collagen type v alpha 2 chain; *col6a1* = collagen type vi alpha 1 chain; *col6a2* = collagen type vi alpha 2 chain; *col11a2* = collagen type xi alpha 2 chain; *col27a1* = collagen type xxvii alpha 1 chain; *col15a1* = collagen type xv alpha 1 chain; VH/CD = villus height to crypt depth.

Disruptions in substance metabolism due to malnutrition in the ileum and jejunum could potentially influence the proliferation of epithelial cells; thereby affecting the morphology of epithelial tissues. In human studies, children with undernutrition enteropathy showed changes in the intestines such as blunting of villi, intestinal barrier dysfunction, and malabsorption of nutrient (Ling et al., 2023). This study notably found that the jejunum was more severely affected by undernutrition compared to the ileum, based on enriched signaling pathways and the quantity of linked DEGs. Particular, ECM-receptor interactions primarily regulated cell adhesion, migration, and proliferation (Leitinger and Hohenester, 2007). Extracellular matrix also induced the activation of FAK and promoted the phosphorylation of PI3K (Shi et al., 2022) that plays a crucial role in cell proliferation, differentiation, and immunity (Zhang et al., 2018). In the current study, DEGs involved in ECM, growth factors, and ECM-receptor interactions were all down-regulated in the jejunal epithelium upon undernutrition, indicating that undernutrition impaired the interactions between the ECM and membrane receptors. Modifications in genes associated with extracellular structure could lead to abnormal signal transduction and potentially lead to disease (Jaalouk and Lammerding, 2009). A previous study reported that undernutrition affected ECM-receptor interaction and inhibited DNA replication and cell cycle progression in ruminal epithelium of pregnant ewes (Xue et al., 2020b). Similarly, ECM-receptor interaction, cell motility, and immune responses were significantly affected in cecal epithelium of ewes in a state of undernutrition (Wu et al., 2023). Results in the current study possibly indicated that undernutrition during late gestation influenced ECM-receptors interaction and some intracellular pathways in jejunal epithelium and affected cell growth and immune responses.

Indeed, it was crucial to acknowledge the limitations of this study. Although a combined analysis of microbiota and epithelium was conducted for the jejunum and ileum using 16S RNA gene sequencing and transcriptome sequencing; which specific bacterium and its metabolites influencing the metabolic homeostasis and functions of jejunal and ileal epithelium upon undernutrition remains unclear. Therefore, it is urgent to explore the precise functions of specific bacteria and their effects on the epithelial metabolism and function, and finally clarify the crosstalk mechanism between microbiota and the host in future studies.

5. Conclusions

In conclusion, our findings suggested that undernutrition in late pregnancy led to a decrease in VFAs and MCP. Undernutrition reduced the relative abundances of *Clostridia UCG-014 norank*, *Ruminococcus*, *[Ruminococcus] gauvreauii*, and *Lachnospiraceae_Blautia* in the jejunum and ileum which were responsible for acetate production. Undernutrition also promoted the up-regulation of genes associated with amino acid synthesis and fatty acid oxidation, and the down-regulation of gene expression pertinent to amino acid degradation, fatty acid synthesis, and extracellular structures in jejunal and ileal epithelium. Alterations in substance transport and metabolism might affect some key signaling transductions, resulting in the downregulation of genes associated with ECM-receptor interactions, cell growth, and immune responses in the jejunal epithelium. Ultimately the jejunum was more impaired in its villus morphology than the ileum (Fig. 8).

These findings revealed the impact of undernutrition on the small intestine microbiota and epithelial tissue during late pregnancy, providing a foundation for the exploration of microbiota–host interactions under malnutrition condition. These insights may help to inform the development of nutritional regulation strategies aimed at alleviating energy shortages in ruminants during late pregnancy.

Credit Author Statement

Weibin Wu: Writing – review & editing, Writing – original draft, Visualization, Validation, Software. **Muhammad Faheem Akhtar:** Writing – review & editing, Writing – original draft, Visualization, Software. **Jiahong Geng:** Writing – review & editing, Writing – original draft, Visualization, Validation, Investigation.

Huizhen Lu: Validation, Supervision, Software. **Muhammad Ajwad Rahim:** Software, Resources. **Jianbo Cheng:** Validation, Methodology, Investigation. **Xiaoling Ding:** Resources, Project administration, Methodology. **Shengyong Mao:** Writing – review & editing, Funding acquisition, Formal analysis, Data curation, Conceptualization. **Yanfeng Xue:** Writing – review & editing, Project administration, Funding acquisition, Formal analysis, Data curation, Conceptualization.

Data availability statement

Raw reads of transcriptome sequencing of jejunal and ileal epithelium are available at GEO, under accession number GSE221270. Raw reads of 16S rRNA gene sequencing are available at the National Center for Biotechnology Information Sequence Read Archive (SRA), under SRA project number PRJNA992195.

Declaration of competing interest

We declare that we have no financial and personal relationships with other people or organizations that can inappropriately influence our work, and there is no professional or other personal interest of any nature or kind in any product, service and/or company that could be construed as influencing the content of this paper.

Acknowledgments

This work was supported by the National Key Research and Development Program of China (2022YFD1301102), Anhui Provincial Natural Science Foundation (2308085QC104), AAU Introduction of High-level Talent Funds (RC392107), and Shandong Province Modern Agricultural Industrial Technology System Project (SDAIT-27).

Appendix A. Supplementary data

Supplementary data to this article can be found online at https://doi.org/10.1016/j.aninu.2024.10.004.

References

Aoac. Official methods of analysis. Arlinton, VA: Official Analytical Chemists; 2000.
Aoac. Official methods of analysis. Washington DC, USA: Official Analytical Chemists; 2016.
Bauer MK, Breier BH, Harding JE, Veldhuis JD, Gluckman PD. The fetal somatotropic axis during long term maternal undernutrition in sheep: evidence for nutritional regulation in utero. Endocrinology 1995;136:1250–7.
Bergman E. Energy contributions of volatile fatty acids from the gastrointestinal tract in various species. Physiol Rev 1990;70:567–90.
Bougarne N, Weyers B, Desmet SJ, Deckers J, Ray DW, Staels B, De Bosscher K. Molecular actions of pparα in lipid metabolism and inflammation. Endocr Rev 2018;39:760–802.
Bradford MM. A rapid and sensitive method for the quantitation of microgram quantities of protein utilizing the principle of protein-dye binding. Anal Biochem 1976;72:248–54.
Cal Pereyra L, Acosta Dibarrat J, Benech A, Da Silva S, Martín A, González Montaña JR. Toxemia de la gestación en ovejas: Revisión. Revista Mexicana De Ciencias Pecuarias 2012;3:247–64.
Cal Pereyra L, González Montaña JR, Benech A, Acosta Dibarrat J, Martín MJ, Perini S, Abreu MC, Da Silva S, Rodríguez P. Evaluation of three therapeutic alternatives for the early treatment of ovine pregnancy toxaemia. Ir Vet J 2015;68:25.
Chilliard Y, Bocquier F, Doreau M. Digestive and metabolic adaptations of ruminants to undernutrition, and consequences on reproduction. Reprod Nutr Dev 1998;38:131–52.
Chomczynski P, Sacchi N. Single step method of rna isolation by acid guanidinium thiocyanate phenol chloroform extraction. Anal Biochem 1987;162:156–9.
Crost EH, Le Gall G, Laverde Gomez JA, Mukhopadhya I, Flint HJ, Juge N. Mechanistic insights into the cross-feeding of ruminococcus gnavus and ruminococcus bromii on host and dietary carbohydrates. Front Microbiol 2018;9:2558.
Da Poian A, El Bacha T, Luz M. Nutrient utilization in humans: metabolism pathways. Nature Education 2010;3:11.
Dekaboruah E, Suryavanshi MV, Chettri D, Verma AK. Human microbiome: an academic update on human body site specific surveillance and its possible role. Arch Microbiol 2020;202:2147–67.
Fattet I, Hovell FDD, Ørskov ER, Kyle DJ, Pennie K, Smart RI. Undernutrition in sheep. The effect of supplementation with protein on protein accretion. Br J Nutr 1984;52:561–74.
Felizardo RJF, Watanabe IKM, Dardi P, Rossoni LV, NOS Câmara. The interplay among gut microbiota, hypertension and kidney diseases: the role of short-chain fatty acids. Pharmacol Res 2019;141:366–77.
Idamokoro E, Muchenje V, Masika P. Peri-and post-parturient consequences of maternal undernutrition of free ranging does: a review. Livest Res Rural Dev 2017;29:202.
Jaalouk DE, Lammerding J. Mechanotransduction gone awry. Nat Rev Mol Cell Biol 2009;10:63–73.
Ji X, Liu N, Wang Y, Ding K, Huang S, Zhang C. Pregnancy toxemia in ewes: a review of molecular metabolic mechanisms and management strategies. Metabolites 2023;13:149.
Jiang P, Stanstrup J, Thymann T, Sangild PT, Dragsted LO. Progressive changes in the plasma metabolome during malnutrition in juvenile pigs. J Proteome Res 2016;15:447–56.
Judkins TC, Archer DL, Kramer DC, Solch RJ. Probiotics, nutrition, and the small intestine. Curr Gastroenterol Rep 2020;22:1–8.
Jung SM, Kim S. In vitro models of the small intestine for studying intestinal diseases. Front Microbiol 2022;12:767038.
Kaiser IH. Metabolic toxemia of late pregnancy: a disease of malnutrition. JAMA 1967;200:185.
Kilkenny C, Browne WJ, Cuthill IC, Emerson M, Altman DG. Improving bioscience research reporting: the arrive guidelines for reporting animal research. J Pharmacol Pharmacother 2010;1:94–9.
Leitinger B, Hohenester E. Mammalian collagen receptors. Matrix Biol 2007;26:146–55.
Ling C, Versloot CJ, Kvissberg MEA, Hu G, Swain N, Horcas Nieto JM, Miraglia E, Thind MK, Farooqui A, Gerding A. Rebalancing of mitochondrial homeostasis through an nad+-sirt1 pathway preserves intestinal barrier function in severe malnutrition. EBioMedicine 2023;96.
Liu S, Lu H, Mao S, Zhang Z, Zhu W, Cheng J, Xue Y. Undernutrition-induced substance metabolism and energy production disorders affected the structure and function of the pituitary gland in a pregnant sheep model. Front Nutr 2023;10.
Lv X, Cui K, Qi M, Wang S, Diao Q, Zhang N. Ruminal microbiota and fermentation in response to dietary protein and energy levels in weaned lambs. Animals 2020;10.
Mohamadipoor Saadatabadi L, Mohammadabadi M, Amiri Ghanatsaman Z, Babenko O, Stavetska R, Kalashnik O, Kucher D, Kochuk Yashchenko O, Asadollahpour Nanaei H. Signature selection analysis reveals candidate genes associated with production traits in iranian sheep breeds. BMC Vet Res 2021;17:1–9.
Molinero N, Conti E, Walker Alan W, Margolles A, Duncan Sylvia H, Delgado S. Survival strategies and metabolic interactions between ruminococcus gauvreauii and ruminococcoides bili, isolated from human bile. Microbiol Spectr 2022;10:e02776-21.
Neuman H, Debelius JW, Knight R, Koren O. Microbial endocrinology: the interplay between the microbiota and the endocrine system. FEMS (Fed Eur Microbiol Soc) Microbiol Rev 2015;39:509–21.
Ogunrinola GA, Oyewale JO, Oshamika OO, Olasehinde GI. The human microbiome and its impacts on health. International Journal of Microbiology 2020;2020.
Oliphant K, Allen Vercoe E. Macronutrient metabolism by the human gut microbiome: major fermentation by-products and their impact on host health. Microbiome 2019;7:91.
Pathak A. Various factors affecting microbial protein synthesis in the rumen. Vet World 2008;1:186.
Patterson GT, Osorio EY, Peniche A, Dann SM, Cordova E, Preidis GA, Suh JH, Ito I, Saldarriaga OA, Loeffelholz M, Ajami NJ, Travi BL, Melby PC. Pathologic inflammation in malnutrition is driven by proinflammatory intestinal microbiota, large intestine barrier dysfunction, and translocation of bacterial lipopolysaccharide. Front Immunol 2022;13.
Penner GB. Mechanisms of volatile fatty acid absorption and metabolism and maintenance of a stable rumen environment. In: 25th Florida ruminant nutrition symposium; 2014. p. 92–104.
Qin W. Determination of rumen volatile fatty acids by means of gas chromatography. Journal of Nanjing Agricultural College 1982;4:110–6.
Ribeiro SA, Braga ELR, Queiroga ML, Clementino MA, Fonseca XMQC, Belém MO, et al. A new murine undernutrition model based on complementary feeding of undernourished children causes damage to the morphofunctional intestinal epithelium barrier. J Nutr 2024;154:1232–51.
Rook JS. Pregnancy toxemia of ewes, does, and beef cows. Vet Clin Food Anim Pract 2000;16:293–317.
Roudbar MA, Abdollahi Arpanahi R, Mehrgardi AA, Mohammadabadi M, Yeganeh AT, Rosa G. Estimation of the variance due to parent of origin effects for productive and reproductive traits in lori bakhtiari sheep. Small Rumin Res 2018;160:95–102.
Rowland I, Gibson G, Heinken A, Scott K, Swann J, Thiele I, Tuohy K. Gut microbiota functions: metabolism of nutrients and other food components. Eur J Nutr 2018;57:1–24.
Safaei SMH, Dadpasand M, Mohammadabadi M, Atashi H, Stavetska R, Klopenko N, Kalashnyk O. An origanum majorana leaf diet influences myogenin gene

expression, performance, and carcass characteristics in lambs. Animals 2022;13:14.
San Juan Vergara H, Zurek E, Ajami NJ, Mogollon C, Peña M, Portnoy I, Vélez JI, Cadena Cruz C, Diaz Olmos Y, Hurtado Gómez L, Sanchez Sit S, Hernández D, Urruchurtu I, Di Ruggiero P, Guardo García E, Torres N, Vidal Orjuela O, Viasus D, Petrosino JF, Cervantes Acosta G. A lachnospiraceae-dominated bacterial signature in the fecal microbiota of hiv-infected individuals from Colombia, south America. Sci Rep 2018;8:4479.
Seth I, Lim B, Cevik J, Gracias D, Chua M, Kenney PS, Rozen WM, Cuomo R. Impact of nutrition on skin wound healing and aesthetic outcomes: a comprehensive narrative review. JPRAS Open 2024;39:291–302.
Shi W, Shang Q, Zhao Y. Spc25 promotes hepatocellular carcinoma metastasis via activating the fak/pi3k/akt signaling pathway through itgb4. Oncol Rep 2022;47:1–14.
Smith SR, Pozefsky T, Chhetri M. Nitrogen and amino acid metabolism in adults with protein-calorie malnutrition. Metabolism 1974;23:603–18.
Thaiss CA, Zmora N, Levy M, Elinav E. The microbiome and innate immunity. Nature 2016;535:65–74.
Turner JR. Intestinal mucosal barrier function in health and disease. Nat Rev Immunol 2009;9:799–809.
Valdes AM, Walter J, Segal E, Spector TD. Role of the gut microbiota in nutrition and health. BMJ 2018;361:k2179.
Wu W, Lu H, Cheng J, Geng Z, Mao S, Xue Y. Undernutrition disrupts cecal microbiota and epithelium interactions, epithelial metabolism, and immune responses in a pregnant sheep model. Microbiol Spectr 2023;11:e05320-22.
Xiong B, Luo Q, Zhou Z, Zhao F. Tables of feed composition and nutritive values in China. 29th ed. Chinese Feed; 2018. p. 81–6.
Xue Y, Hu F, Guo C, Mei S, Xie F, Zeng H, Mao S. Undernutrition shifted colonic fermentation and digest-associated bacterial communities in pregnant ewes. Appl Microbiol Biotechnol 2020a;104:5973–84.
Xue Y, Lin L, Hu F, Zhu W, Mao S. Disruption of ruminal homeostasis by malnutrition involved in systemic ruminal microbiota-host interactions in a pregnant sheep model. Microbiome 2020b;8:138.
Zhang H, Hu J, Fu R, Liu X, Zhang Y, Li J, Liu L, Li Y, Deng Q, Luo Q. Flavonoids inhibit cell proliferation and induce apoptosis and autophagy through downregulation of pi3kγ mediated pi3k/akt/mtor/p70s6k/ulk signaling pathway in human breast cancer cells. Sci Rep 2018;8:11255.
Zhang S, Lv Y, Qian J, Wei W, Zhu Y, Liu Y, Li L, Zhao C, Gao X, Yang Y, Dong J, Gu Y, Chen Y, Sun Q, Jiao X, Lu J, Yan Z, Wang L, Yuan N, Fang Y, Wang J. Adaptive metabolic response to short-term intensive fasting. Clin Nutr 2024;43:453–67.
Zoetendal EG, Akkermans AD, De Vos WM. Temperature gradient gel electrophoresis analysis of 16s rrna from human fecal samples reveals stable and host-specific communities of active bacteria. Appl Environ Microbiol 1998;64:3854–9.